0026-895X/05/6704-1137–1144$20.00
MOLECULAR PHARMACOLOGY
Copyright © 2005 The American Society for Pharmacology and Experimental Therapeutics
Mol Pharmacol 67:1137–1144, 2005

Vol. 67, No. 4
4275/1196371
Printed in U.S.A.

A Novel Class of Fusion Polypeptides Inhibits Exocytosis

Kenji Matsushita, Craig N. Morrell, and Charles J. Lowenstein

Departments of Medicine (K.M., C.J.L.), Pathology (C.N.M., C.J.L.), and Comparative Medicine (C.N.M.), The Johns Hopkins University School of Medicine, Baltimore, Maryland

Received June 25, 2004; accepted December 17, 2004

ABSTRACT

N-Ethyl-maleimide–sensitive factor (NSF) plays a critical role in the regulation of exocytosis. NSF regulates exocytosis by interacting with a complex containing soluble NSF attachment protein receptor (SNARE) molecules, hydrolyzing ATP, and disassembling the SNARE complex. We hypothesized that peptide inhibitors of NSF would decrease exocytosis. We now report the development of a novel set of peptides that block exocytosis by inhibiting NSF activity. These NSF inhibitors are fusion polypeptides composed of an 11 amino acid human immunodeficiency virus transactivating regulatory protein (TAT) domain fused to a 22 amino acid NSF domain. These TAT-NSF fusion polypeptides cross endothelial cell membranes, inhibit NSF hydrolysis of ATP, decrease NSF disassembly of SNARE molecules, and block exocytosis of von Willebrand factor. Control peptides have no effect on exocytosis. TAT-NSF inhibitors administered to mice prolong the bleeding time. Blood concentrations of these TAT-NSF peptides rapidly decrease within 5 min after injection and then remain constant from 10 to 60 min after injection. These TAT-NSF compounds may be useful in the treatment of a variety of diseases in which exocytosis plays a prominent role, including myocardial infarction, stroke, thrombosis, and autoimmune disorders.

Exocytosis plays a prominent role in cell biology. A variety of cell types respond to extracellular stimuli by releasing the contents of vesicle or granules to the external environment. For example, depolarizing neurons trigger exocytosis of neurovesicles, releasing neurotransmitters that activate postsynaptic neurons. Adrenal chromaffin cells respond to external signals such as histamine, angiotensin II, and opioids by exocytosis of chromaffin granules containing catecholamines and other components. Endothelial cells respond to a variety of signals, including thrombin, histamine, and ATP by exocytosis of Weibel-Palade bodies (Birch et al., 1994; Foreman et al., 1994; Datta et al., 1995; Vischer et al., 1995; Vischer and Wollheim, 1997). Weibel-Palade bodies are endothelial granules that contain von Willebrand factor (vWF), P-selectin, and interleukin-8 (Wagner, 1993; Utgaard et al., 1998; Wolff et al., 1998). Because vWF causes platelet aggregation, P-selectin promotes neutrophil adherence to vessel walls, and interleukin-8 attracts and activates neutrophils, the contents of Weibel-Palade bodies can promote vascular inflammation and thrombosis.

We recently showed that endothelial exocytosis is regulated in part by the cellular machinery that regulates vesicle trafficking, including SNAREs, NSF, Rab, Munc, and other accessory proteins (Matsushita et al., 2003). Soluble NSF attachment protein receptors (SNAREs) are transmembrane proteins that regulate vesicle fusion (Ferro-Novick and Jahn, 1994). Vesicle SNAREs are localized to vesicle membranes, and target SNAREs are localized to target membranes (Sollner et al., 1993a). A set of three SNARE molecules assembles into a stable ternary complex, bringing the vesicle into apposition with a target membrane (Weber et al., 1998). SNARE assemble and disassembly play an important role in the cycle of vesicle and granule exocytosis.

SNARE disassembly is regulated by *N*-ethyl-maleimide–sensitive factor (NSF). Rothman and colleagues (Block et al., 1988; Malhotra et al., 1988; Rothman, 1994) discovered NSF as an 85-kDa protein that regulates vesicle fusion and is inhibited by *N*-ethyl-maleimide. Each of the three domains of NSF has a specific function. The N-terminal domain of NSF interacts indirectly with SNARE proteins via soluble NSF attachment proteins (SNAP). The D1 domain of NSF hydro-

This work was supported by National Institutes of Health grants R01-HL63706, R01-HL074061, P01-HL65608, P01-HL56091, and HL78635, American Heart Association grant EIG 0140210N, the Ciccarone Center, and the John and Cora H. Davis Foundation (to C.J.L.); and by National Institutes of Health grants RR07002 and HL074945 (to C.M.).

Article, publication date, and citation information can be found at http://molpharm.aspetjournals.org.

doi:10.1124/mol.104.004275.

ABBREVIATIONS: vWF, von Willebrand factor; NSF, *N*-ethyl-maleimide–sensitive factor; SNARE, soluble *N*-ethylmaleimide–sensitive factor attachment protein receptor; SNAP, soluble *N*-ethylmaleimide–sensitive factor attachment proteins; TAT, transactivating regulatory protein; RGS, regulator of G protein signaling; FITC, fluorescein isothiocyanate; GST, glutathione *S*-transferase; HAEC, Human aortic endothelial cell; ELISA, enzyme-linked immunosorbent assay; FACS, fluorescence-activated cell sorting; VAMP, vesicle-associated membrane protein; PBS, phosphate-buffered saline.

lyzes ATP and alters the conformation of the ternary SNARE complex, the D2 domain of NSF that regulates NSF oligomerization (Tagaya et al., 1993; Whiteheart et al., 1994; Nagiec et al., 1995; Matveeva et al., 1997; Steel and Morgan, 1998; May et al., 1999; Whiteheart et al., 2001). The critical role that NSF plays in exocytosis is emphasized by the *Drosophila melanogaster* mutant *comatose*; this fly has a temperature-sensitive mutation of the *D. melanogaster* NSF homolog that blocks synaptic transmission, resulting in paralysis at an elevated temperature (Pallanck et al., 1995).

We showed recently that NSF regulates exocytosis of endothelial granules (Matsushita et al., 2003). Furthermore, we discovered that nitric oxide (NO) regulates exocytosis by chemically modifying NSF (Matsushita et al., 2003). From these observations, we hypothesized that inhibitors of NSF would block exocytosis. We now report the design and testing of a novel set of inhibitors that block exocytosis of endothelial granules by inhibiting NSF.

Materials and Methods

Materials. Thrombin was purchased from Enzyme Research Laboratories Inc. (South Bend, IN). Mouse monoclonal antibody to NSF was from BD Biosciences Discovery Labware (Bedford, MA). cDNAs of RGS-His_6-NSF and RGS-His_6-α-SNAP were generous gifts from James E. Rothman (Rockefeller University, New York, NY). Mice were purchased from The Jackson Laboratory (Bar Harbor, ME).

Peptides. Peptides were synthesized by Anaspec Inc. (San Jose, CA). The TAT-NSF57 fusion polypeptide sequence is YGRKKRRQRRR-GGG-GSVAFSLPQRKWAGLSIGQE. The TAT-NSF81 fusion polypeptide sequence is YGRKKRRQRRR-GGG-ALYSFDKAKQCIGTM-TIEID. The TAT-NSF222 fusion polypeptide sequence is YGRKKRRQRRR-GGG-LDKEFNSIFRRAFASRVFPPE. The TAT-NSF254 fusion polypeptide sequence is YGRKKRRQRRR-GGG-KGILLYGPPGCGKTLLARQIG. The TAT-NSF700 fusion polypeptide sequence is YGRKKRRQRRR-GGG-LLDYVPIGPRFSNLVLQALLVL. These peptides were labeled with FITC using a FITC-labeling kit (Calbiochem, San Diego, CA) for some experiments. As controls, scrambled peptides were also synthesized; these peptides contained the intact TAT domain followed by the amino acid residues of the NSF domain in a random order. The TAT-NSF57scr fusion polypeptide sequence is YGRKKRRQRRR-GGG-LSFGVGSAKEISRQAQWPLG. The TAT-NSF81scr fusion polypeptide sequence is YGRKKRRQRRR-GGG-QDGCKYFATDETIMKLSIAI. The TAT-NSF222scr fusion polypeptide sequence is YGRKKRRQRRR-GGG-GENSFRFLADIFPAKAFPVRFE. The TAT-NSF254scr fusion polypeptide sequence is YGRKKRRQRRR-GG-AIMLPNEAGKRLTQRLKGK. The TAT-NSF700scr fusion polypeptide sequences is YGRKKRRQRRR-GGG-GIPPVYFSRLDLN-LVVLLLAQL.

Preparation of Recombinant NSF and SNARE Polypeptides. Recombinant RGS-His_6-NSF and RGS-His_6-α-SNAP were expressed in bacteria and purified on a nickel-nitrilotriacetic acid–agarose column (HisTRAP; Amersham Biosciences AB, Uppsala, Sweden). Recombinant GST-SNARE proteins were expressed in BL21 cells and purified with glutathione-agarose (GSTrap; Amersham). For some assays, the GST tag was cleaved off of the GST-SNARE polypeptide with thrombin.

Cell Culture and Analysis of vWF Release. Human aortic endothelial cells (HAECs) and endothelial growth medium-2 media were obtained from Cambrex Bio Science Walkersville (Walkersville, MD). HAECs were pretreated with TAT-NSF peptides, washed, and stimulated with 1 U/ml thrombin, and the amount of vWF released into the media was measured by ELISA (American Diagnostica, Greenwich, CT).

Cell Culture and Analysis of Insulin Release

The Rat Insulinoma Cell Line. RIN-m5F and RPMI 1640 media were obtained from American Type Culture Collection (Manassas, VA). RIN-m5F cells were starved with low concentration of D-glucose (2.8 mM) in Hanks' balanced salt solution for 2 h, pretreated with TAT-peptides for 20 min, washed, and then stimulated with high concentrations of D-glucose (28 mM) in Hanks' balanced salt solution for 1 h. The amount of insulin released into the media was measured by an insulin ELISA kit (Crystal Chemical Inc., Downers Grove, IL).

Entry of TAT-NSF Peptides into Endothelial Cells. HAECs were incubated with 10 μM FITC-labeled TAT-NSF peptides for 20 min and treated with 200 μg/ml ethidium bromide to quench extracellular FITC, and fluorescence was measured in a Cytofluor 2300 fluorometer (Millipore Corporation, Billerica, MA). FITC-positive cells were measured by FACS analysis.

ATPase Assay. The ATPase activity of NSF was measured by a coupled assay, in which ATP use is linked to the pyruvate kinase reaction, which generates pyruvate, which in turn is measured continuously with lactate dehydrogenase (Huang and Hackney, 1994). Recombinant NSF (0.2 μg/μl) was pretreated with buffer or TAT-NSF peptide for 10 min at 22°C. ATPase reaction buffer (100 mM HEPES buffer, pH 7.0, 100 mM KCl, 10 mM $MgCl_2$, 5 mM $CaCl_2$, 10 mM ATP, 5 mM phosphoenol pyruvate, 50 U of lactate dehydrogenase, and 50 U of pyruvate kinase) was added to the mixture, followed by 10 μl of NADH (2 mg/ml in 1% sodium bicarbonate). The mixture was incubated for 10 min at 22°C, and the absorbance was measured at 340 nm.

NSF Disassembly Assay. Analysis of the 7S and 20S complexes was performed according to protocols published previously (Sollner et al., 1993b). The disassembly activity of NSF was measured by a coprecipitation assay (Pevsner et al., 1994). Recombinant RGS-His_6-NSF (0.1 μg/μl) was pretreated with buffer or TAT-NSF peptides for 10 min at 22°C. Recombinant RGS-His_6-α-SNAP (0.1 μg/μl) and SNARE polypeptides (0.1 μg/μl each of VAMP-3, SNAP-23, and GST-syntaxin-4) were added, followed by either 5 mM ATP/10 mM $MgCl_2$ or 5 mM ATP-γS/10 mM $MgCl_2$. This mixture of NSF and SNARE polypeptides was then incubated in binding buffer (4 mM HEPES, pH 7.4, 0.1M NaCl, 1 mM EDTA, 3.5 mM $CaCl_2$, 3.5 mM $MgCl_2$, and 0.5% Nonidet P-40) and glutathione-Sepharose beads for 1 h at 4°C with rotation. The beads were washed with binding buffer four times, mixed with SDS-polyacrylamide gel electrophoresis sample buffer, boiled for 3 min, and analyzed by immunoblotting.

Bleeding Times in Mice. Measurement of bleeding time in mice was performed as described previously (Weiss et al., 2002). Mice were anesthetized with an intramuscular injection of ketamine and xylazine, and 5 mm of the distal tip of the tail was amputated. The tail was blotted with filter paper every 5 s until the paper was no longer stained. If the animals bled for 20 min, the experiment was stopped, and the bleeding time was recorded as 20 min.

Bioavailability of TAT-NSF Peptides in Mice. Mice were injected intravenously with PBS, FITC alone, or 0.5 mg/kg FITC-TAT-NSF peptides. At various times after injection of the peptide, the distal tip of the tail was amputated, and blood was collected. Fluorescence in the blood were measured by fluorometry.

Statistics. The EC_{50} for the TAT-NSF peptide inhibition of thrombin-activated exocytosis from endothelial cells was calculated using the Marquardt algorithm.

Results

Design of Peptide Inhibitors of NSF. We designed a set of fusion polypeptide inhibitors of NSF (Table 1). The amino terminus of all fusion peptides is an 11 amino acid residue polypeptide fragment derived from the human immunodeficiency virus TAT domain (YGRKKRRQRRR). This domain can efficiently deliver peptides and polypeptides into cells via lipid raft macropinocytosis (Schwarze et al., 1999; Vocero-

Akbani et al., 2000, 2001; Becker-Hapak et al., 2001; Wadia et al., 2004). The amino terminal domain is followed by a linker domain consisting of GGG. The carboxyl terminus of each fusion peptide is derived from unique domains of NSF. We selected NSF domains of 20 to 25 amino acid residues from regions that we or others had shown by mutagenesis are critical for NSF function (Table 1). We predicted that these fragments of NSF would inhibit specific NSF activities, such as NSF ATPase activity, NSF disassembly of SNAREs, or NSF homohexamerization (Table 1).

Using these principles of design, we synthesized a set of five fusion polypeptide inhibitors of NSF. The peptides are referred to as TAT-NSF fusion peptides and are identified with a number corresponding to the amino-terminal amino acid residue of NSF. For example, TAT-NSF222 is composed of 11 amino acids of the human immunodeficiency virus TAT polypeptide (YGRKKRRQRRR), followed by 3 amino acids as a linker (GGG), followed by 23 amino acids of the NSF D1 domain, residues 222 to 243 (LDKEFNSIFRRAFASRVFPPE). The sequence of the entire fusion peptide designated TAT-NSF222 is YGRKKRRQRRR-GGG-LDKEFNSIFRRAFASRVFPPE.

We also designed a set of control TAT-NSF peptides. These peptides are composed of the intact TAT domain followed by a domain containing the TAT amino acid residues in a scrambled order. These peptides are referred to as TAT-NSFscr. For example, TAT-NSF57scr contains the TAT domain fused to the 22 amino acids of NSF from 57 to 77 in a scrambled order. We then measured the effect of the active and control peptides upon NSF activities and exocytosis.

TAT-NSF Peptides Inhibit Weibel-Palade Body Exocytosis. We first explored the effect of TAT-NSF peptides upon endothelial exocytosis. We incubated HAECs for 20 min with increasing concentrations of each of the five TAT-NSF peptides: TAT-NSF57, TAT-NSF-81, TAT-NSF222, TAT-NSF254, and TAT-NSF700. HAECs were then treated with thrombin, and the amount of vWF released into the media was measured by ELISA. TAT-NSF peptides inhibit vWF release in a dose-dependent manner (Fig. 1A). For TAT-NSF57 the EC_{50} = 488 μM (R^2 = 0.999); for TAT-NSF81, the EC_{50} = 1.9 μM (R^2 = 0.999); for TAT-NSF222 the EC_{50} = 4.9 μM (R^2 = 0.996); for TAT-NSF254 the EC_{50} = 107 μM (R^2 = 0.999); and for TAT-NSF700 the EC_{50} = 0.2 μM (R^2 = 0.999). We then repeated these experiments using the control peptides. TAT-NSF–scrambled peptides have no effect on endothelial exocytosis (Fig. 1B).

We examined the dose response of TAT-NSF81 and TAT-NSF700 in more detail. TAT-NSF81 inhibits thrombin-induced exocytosis of endothelial cells in a dose-responsive manner (Fig. 1C). TAT-NSF700 inhibits thrombin-induced exocytosis of endothelial cells in a dose-responsive manner (Fig. 1C).

We then explored the effect of TAT-NSF81 and TAT-NSF700 upon insulin release from a rat insulinoma cell line. Pancreatic islet cells release insulin by regulated exocytosis; we hypothesized that TAT-NSF polypeptides would inhibit insulin release. Therefore, we treated the rat insulinoma cell line RIN-m5F with increasing amounts of TAT-NSF81 or TAT-NSF700. The insulinoma cells were then exposed to low levels of glucose (2.8 mM) or high levels of glucose (28 mM) for 1 h, and the amount of insulin released into the media was measured by ELISA. Nontreated RIN-m5F cells release basal levels of insulin at low levels of glucose, and high glucose stimulates an additional release of insulin (Fig. 1D). The TAT-NSF peptides inhibit glucose stimulation of insulin release (Fig. 1D). These data show that TAT-NSF peptides are inhibitors of endothelial exocytosis.

TAT-NSF Entry into Endothelial Cells. TAT peptides enter cells by the process of macropinocytosis (Wadia et al., 2004). We measured the entry of TAT-NSF peptides into endothelial cells using FITC-labeled TAT-NSF peptides. We first added equal concentrations of FITC-TAT-NSF peptides to wells containing media but no cells and measured the fluorescence. There is a slight difference in the fluorescence of each peptide (Fig. 2A, □). We then added equal concentrations of FITC-TAT-NSF peptides to endothelial cells, and after 20 min, we washed the cells and measured fluorescence. After 20 min, endothelial cells contained slightly different concentrations of FITC-TAT-NSF peptides (Fig. 2A, ■). HAEC cells contain higher concentrations of TAT-NSF57 and TAT-NSF700 and lower concentrations of the other peptides.

We also measured the percentage of endothelial cells that had been transduced with the FITC-TAT-NSF peptides. HAECs were incubated with FITC-TAT-NSF peptides, and the fluorescence of the cells was measured by FACS. Most TAT-NSF peptides transduce approximately 75% of endothelial cells within 20 min (Fig. 2B). However, TAT-NSF57 transduces approximately 50% of cells within 20 min. As a negative control, we confirmed that extracellular ethidium bromide quenches the fluorescence of FITC-TAT-NSF peptides (Fig. 2C). These data show that the fluorescence of FITC-TAT-NSF peptides varies between peptides, that most peptides can transduce the same percentage of endothelial cells, but concentrations of peptides within cells varies between peptides.

Selected TAT-NSF Peptides Inhibit NSF ATPase Activity. We next explored the effect of TAT-NSF peptides upon NSF ATPase activity. The ATPase activity of NSF is necessary for NSF to disassemble SNARE complexes and regulate exocytosis. We designed the TAT-NSF222 and TAT-

TABLE 1

Design of TAT-NSF polypeptides

All TAT-NSF fusion polypeptides contain the TAT domain YGRKKRRQRRR followed by a linker GGG followed by a unique NSF domain. The NSF domains were selected on the basis of studies of the structure and function of NSF.

ID	Position	NSF Sequence	Rationale
TAT-NSF57	57–77	GSVAFSLPQRKWAGLSIGQE	R67E SNAP binding
TAT-NSF81	81–101	ALYSFDKAKQCIGTMTIEID	C91 NO Target
TAT-NSF222	222–243	LDKEFNSIFRRAFASRVFPPE	Disassembly
TAT-NSF254	254–274	KGILLYGPPGCGKTLLARQIG	C264 disassembly Comatose mutant G260
TAT-NSF700	700–720	LLDYVPIGPRFSNLVLQALLVL	Hexamerization mutants

NSF254 polypeptides to contain regions of NSF adjacent to or within NSF domains that mediate ATP hydrolysis (Dalal and Hanson, 2001). We then tested the ability of these and other peptides to inhibit NSF ATPase activity.

Recombinant NSF was incubated with 10 μM TAT-NSF peptides, and ATPase activity was measured by a coupled assay (Huang and Hackney, 1994). Some of the TAT-NSF peptides have no effect upon NSF ATPase activity, and others have a more pronounced inhibition of NSF ATPase activity (Fig. 3A). In particular, TAT-NSF81, TAT-NSF222, and TAT-NSF700 all inhibit NSF hydrolysis of ATP. The two peptides designed to inhibit NSF ATP hydrolysis are less effective than two other peptides that contain NSF domains far from the two regions known to bind and hydrolyze ATP (Fig. 3A). We further defined TAT-NSF81 and TAT-NSF700 inhibition of NSF ATP hydrolysis. TAT-NSF81 and TAT-NSF700 inhibit NSF ATPase activity in a dose-responsive manner (Fig. 3B).

TAT-NSF Peptides Inhibit NSF Disassembly Activity. We next explored the effect of TAT-NSF peptides upon NSF disassembly activity. For NSF to disassemble the SNARE complex, the N-terminal domain of NSF interacts with the SNARE complex via α-SNAP, and then NSF uses the chemical energy from ATP hydrolysis to physically separate the SNARE molecules. We designed TAT-NSF57 and TAT-NSF81 to contain regions of the N-terminal domain of NSF that would interfere with NSF disassembly of SNARE complexes.

To measure the effects of TAT-NSF peptides upon NSF disassembly activity, we expressed in bacteria and purified recombinant His_6-NSF, His_6-α-SNAP, and three SNARE molecules found in endothelial cells GST-syntaxin-4, VAMP-3, and SNAP-23 (Matsushita et al., 2003). We then used a coprecipitation assay to measure the interaction between NSF and SNAREs. In this assay, we pulled down the SNARE syntaxin-4 and determined whether NSF precipitates along with syntaxin-4. As controls, we add ATP or ATP-γS. ATP-γS locks NSF onto the SNARE complex; precipitation of syntaxin will also pull down NSF in the presence of ATP-γS. In contrast, ATP permits NSF to separate from the SNARE complex; precipitation of syntaxin will not pull down NSF in the presence of ATP.

Recombinant His_6-NSF was mixed with α-SNAP, GST-syntaxin, VAMP-3, and SNAP-23. ATP or ATP-γS was added, the mixture was precipitated with glutathione-Sepharose beads, and precipitants were immunoblotted with antibody to the NSF His_6 tag. As expected, ATP permits NSF to release SNARE molecules, and NSF does not coprecipitate

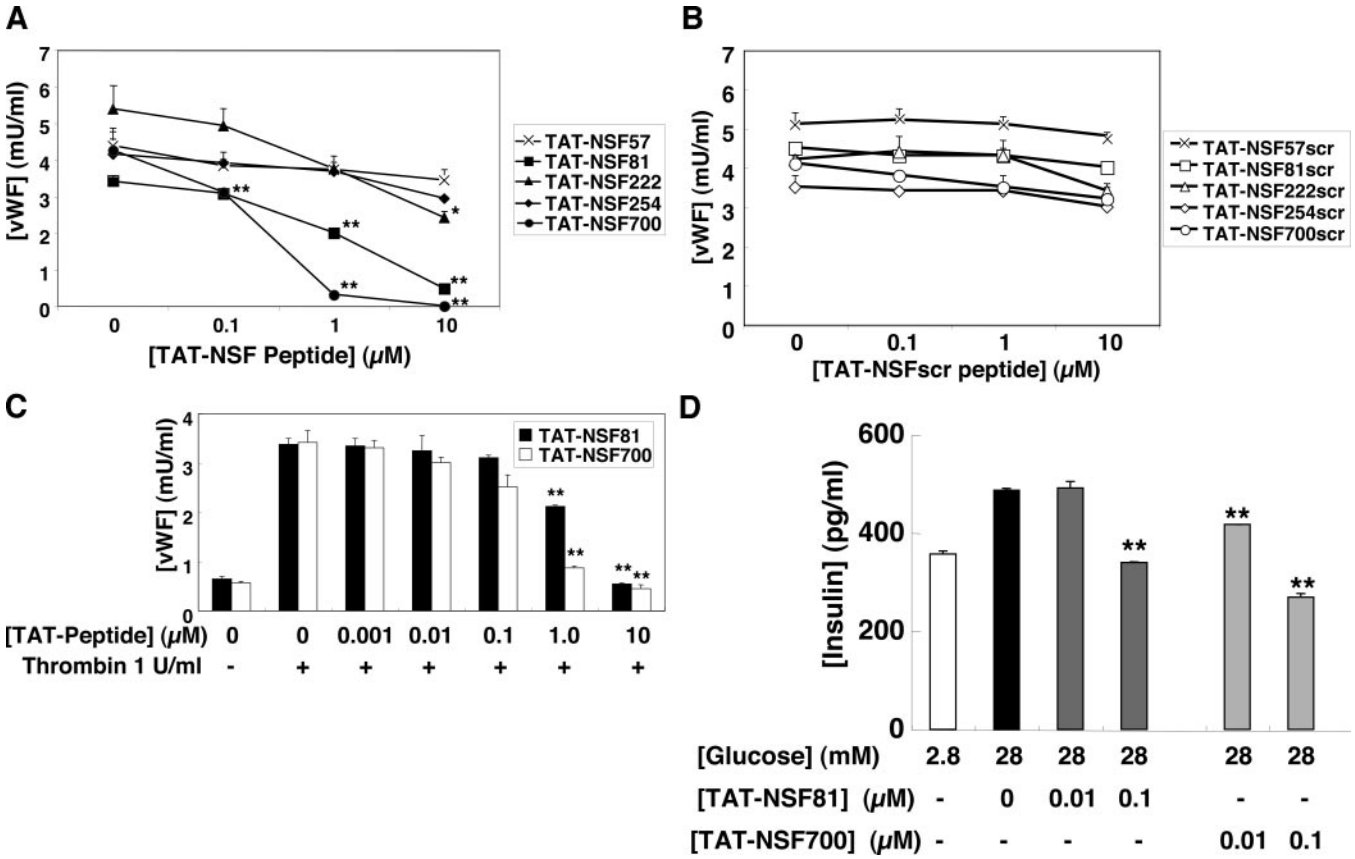

Fig. 1. TAT-NSF peptide inhibition of exocytosis. A, TAT-NSF peptides inhibit thrombin-induced exocytosis from HAECs. HAECs were pretreated with TAT-NSF peptides for 20 min and then treated with thrombin, and the amount of vWF released into the media was measured by ELISA (n = 3 ± S.D; ⋆, $P < 0.05$ versus 0 μM; ⋆⋆, $P < 0.01$ versus 0 μM). B, scrambled TAT-NSF control peptides do not inhibit thrombin-induced exocytosis from HAECs. HAECs were pretreated with scrambled TAT-NSF peptides for 20 min and then treated with thrombin, and the amount of vWF released into the media was measured by ELISA (n = 3 ± S.D.). C, dose-response effect of TAT-NSF81 and TAT-NSF700 on thrombin-induced exocytosis from HAECs. HAECs were pretreated with TAT-NSF81 for 20 min and then treated with thrombin, and the amount of vWF released into the media was measured by ELISA (n = 3 ± S.D.; ⋆⋆, $P < 0.01$ versus 0 μM). D, effect of TAT-NSF81 and NSF700 on insulin exocytosis from rat insulinoma cells. RIN-m5F cells were pretreated with TAT-NSF81 or TAT-NSF700 for 20 min and then treated with 28 mM glucose for 1 h, and the amount of insulin released into the media was measured by ELISA (n = 3 ± S.D.; ⋆⋆, $P < 0.01$ versus 0 μM).

with SNAREs (Fig. 4A, lane 1). Also as expected, ATP-γS locks NSF onto the SNARE complex, and NSF coprecipitates with SNAREs (Fig. 4A, lane 2).

We next added 1 μM individual TAT-NSF peptides to recombinant NSF, α-SNAP, and SNAREs and then precipitated SNAREs and immunoblotted the precipitants with antibody to the NSF tag. All TAT-NSF peptides inhibit NSF disassociation from the SNARE complex (Fig. 4A). TAT-NSF81 is particularly effective at blocking NSF disassembly activity. A dose-response measurement shows that for TAT-NSF81, the EC_{50} = 0.1 to 1.0 μM (Fig. 4B). The control peptide TAT-NSF81scr had no effect (Fig. 4C). A dose-response measurement shows that for TAT-NSF700, the EC_{50} = 1.0 to 10 μM (Fig. 4D). The control peptide TAT-NSF700scr had no effect (Fig. 4E). Taken together, these data show that TAT-NSF peptides inhibit NSF disassembly activity.

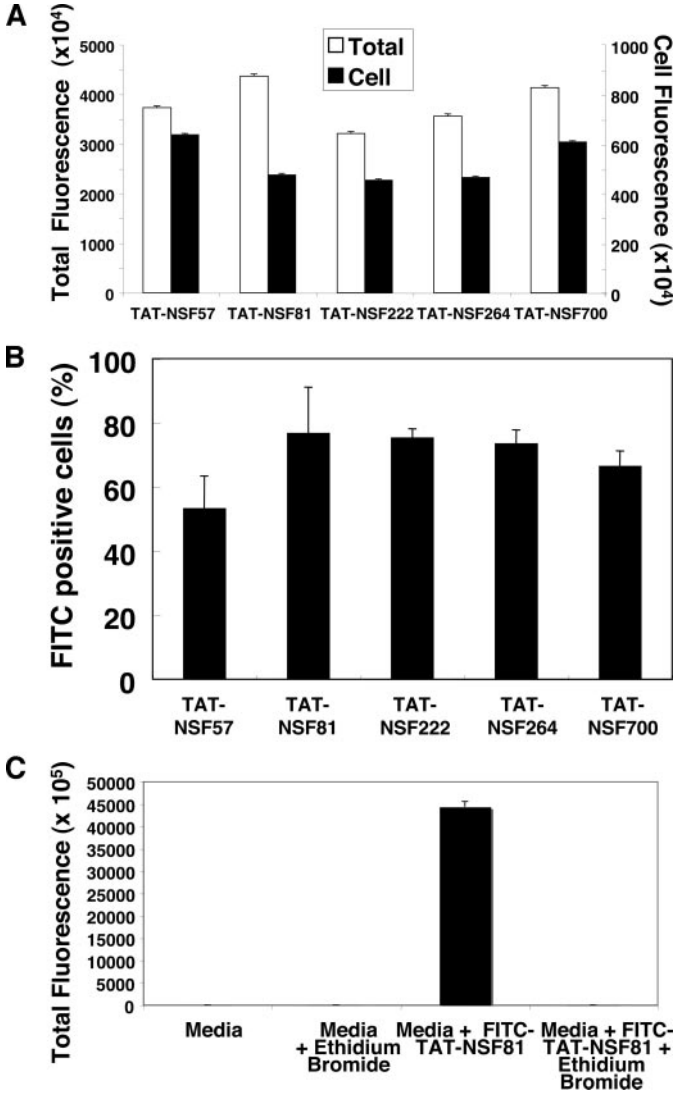

Fig. 2. TAT-NSF peptide entry into cells. A, concentration of FITC-TAT-NSF peptides in HAECs. Cells were incubated with 10 μM FITC-labeled TAT-NSF peptides for 20 min, treated with ethidium bromide to quench extracellular FITC, and cell fluorescence was measured in a fluorometer (■, $n = 5 \pm$ S.D.). Total fluorescence was measured by adding 10 μM FITC-TAT-NSF peptide to wells containing media but no cells (□, $n = 5 \pm$ S.D.). B, percentage of HAEC cells transduced with FITC-TAT-NSF peptides. Cells were incubated with 10 μM FITC-labeled TAT-NSF peptides for 20 min, treated with ethidium bromide to quench extracellular FITC, and imaged by FACS ($n = 3 \pm$ S.D.). C, extracellular ethidium bromide quenches FITC-TAT-NSF fluorescence. FITC-TAT-NSF81 10 μM was incubated with ethidium bromide in media in the absence of cells, and fluorescence was measured in a fluorometer ($n = 3 \pm$ S.D.).

TAT-NSF Peptides Prolong Bleeding Time in Vivo. To test whether TAT-NSF peptides have an effect on exocytosis in vivo, we measured the effect of TAT-NSF peptides on the bleeding time of mice. Thrombosis depends in part on endothelial exocytosis of vWF, which interacts with the platelet glycoprotein Ib-IX-V receptor complex to mediate platelet adherence to the vessel wall (Ruggeri, 2002). We hypothesized that TAT-NSF peptides would decrease endothelial exocytosis, decrease the endothelial release of vWF, decrease platelet adherence, and prolong the bleeding time.

We anesthetized mice and injected them intravenously with saline or TAT-NSF peptides. After 45 min, the distal 5 mm of tail was amputated and the bleeding time measured. If the animals bled continuously for more than 20 min, the bleeding time was recorded as 20 min and the experiment was stopped. Treatment with saline had no effect on the bleeding time (Fig. 5A). In contrast, treatment with the TAT-NSF peptides prolonged the bleeding time (Fig. 5A). Mice treated with saline had a bleeding time of approximately 5 min. TAT-NSF81 at higher doses such as 25 mg/kg prolonged the bleeding time to approximately 15 min. TAT-NSF57 at similar doses prolonged the bleeding time more than 20 min. The most potent peptide, TAT-NSF700, prolonged the bleeding time more than 20 min at lower doses such as 0.25 mg/kg. We also measured the effect of the TAT-NSF700 peptide upon the prothrombin time, the partial thromboplastin time, and the platelet count. TAT-NSF700 2.5 mg/kg had no effect

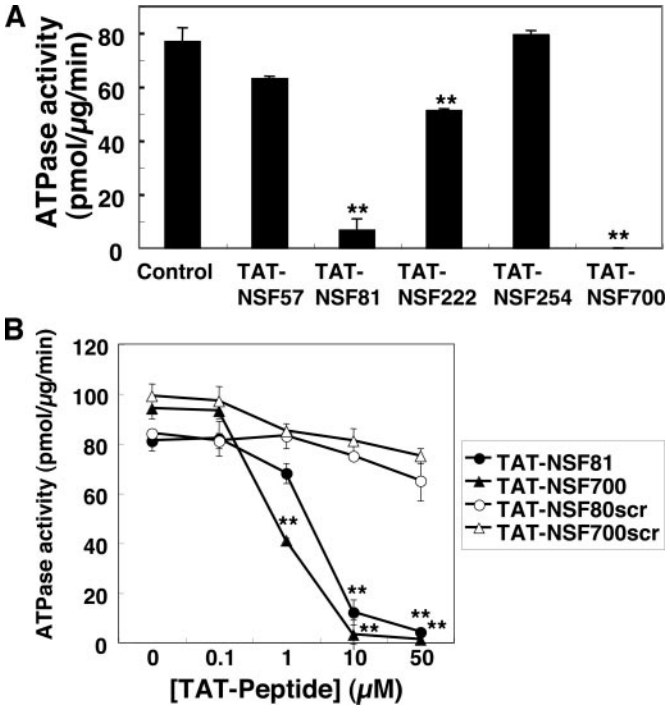

Fig. 3. TAT-NSF peptide inhibition of NSF ATPase activity. A, TAT-NSF peptides inhibit NSF ATPase activity. A colorimetric assay was used to measure the ATPase activity of recombinant NSF that had been treated with 10 μM TAT-NSF peptides ($n = 3 \pm$ S.D.; ⋆⋆, $P < 0.01$ versus control). B, TAT-NSF81 and TAT-NSF700 inhibit NSF ATPase activity. A colorimetric assay was used to measure the ATPase activity of recombinant NSF that had been treated with TAT-NSF81 or TAT-NSF81scr, TAT-NSF700, or TAT-NSF700scr ($n = 3 \pm$ S.D.; ⋆⋆, $P < 0.01$ versus 0 μM).

on the prothrombin time, partial thromboplastin time, or platelet count (data not shown).

We next measured the change over time in blood levels of FITC-labeled TAT-NSF in mice. We injected PBS, FITC, or 0.5 mg/kg FITC-TAT-NSF peptides into mice, collected blood at various times, and measured the fluorescence of the blood. Blood from mice injected with PBS has minimal fluorescence (Fig. 5B, △). Fluorescence of blood from mice injected with FITC-TAT-NSF peptides decreased rapidly within the first 5 min and then remained constant 10 to 60 min after injection (Fig. 5B). These data show that TAT-NSF peptides prolong the bleeding time in vivo and suggest that NSF is a novel target for treatment of thrombotic diseases.

Discussion

The major finding of this study is that novel fusion polypeptides can inhibit exocytosis. Fusion polypeptides composed of a TAT protein transduction domain joined to an NSF domain can enter endothelial cells, inhibit specific NSF activities, and block exocytosis.

How Do TAT-NSF Peptides Inhibit NSF? We used rationale drug design to construct a set of polypeptides that would inhibit NSF. The carboxyl terminal region of each peptide contains a unique 22 amino acid residue domain of NSF. We selected each NSF domain on the basis of structure-function studies of NSF by us and others (Table 1). NSF has at least three major functions: hydrolysis of ATP, disassembly of SNAREs, and homohexamerization.

We designed 2 TAT-NSF polypeptides to interfere with NSF hydrolysis of ATP. TAT-NSF222 and TAT-NSF254 contain regions of NSF adjacent to or within NSF domains that mediate ATP binding and hydrolysis (Dalal and Hanson, 2001). TAT-NSF222 contains an NSF domain extending from residues 222 to 243, which is directly amino-terminal of the Walker A motif of the D1 domain of NSF. TAT-NSF254 contains the NSF domain extending from residues 254 to 274, which includes the Walker A motif of the NSF D1 domain. Our ATPase assay shows that TAT-NSF222 does indeed inhibit NSF ATPase activity (Fig. 3). However, TAT-NSF81 and TAT-NSF700 inhibit NSF ATPase activity even more than the two other peptides specifically targeted to the ATPase domains.

We designed two TAT-NSF polypeptides to block NSF disassembly of SNARE molecules. TAT-NSF57 contains a region of NSF that interacts with the adaptor molecule α-SNAP that in turn interacts directly with SNAREs. TAT-NSF81 contains a cysteine residue that mediates NO inhibition of NSF disassembly. TAT-NSF81 is more effective than TAT-

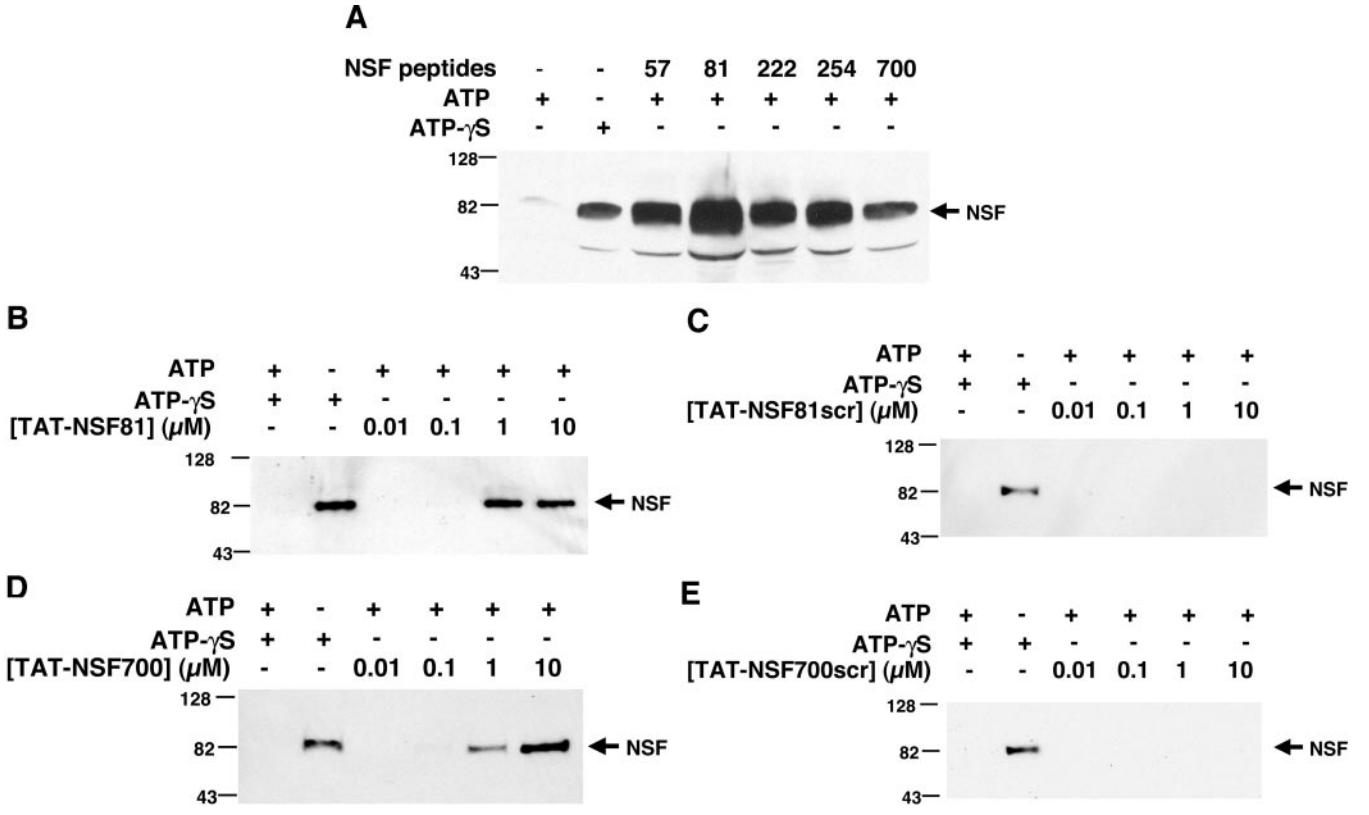

Fig. 4. TAT-NSF peptide inhibition of NSF disassembly activity. A, TAT-NSF peptides inhibit NSF disassembly activity. His_6-NSF was pretreated or not with 1 μM TAT-NSF peptides and then incubated with recombinant α-SNAP and recombinant SNARE molecules GST-syntaxin-4, VAMP-3, and SNAP-23. ATP or ATP-γS was added, and the mixture was precipitated with glutathione-Sepharose. Precipitated proteins were immunoblotted with antibody to the NSF His_6 tag. NSF peptides block the ability of NSF to disassociate from SNARE polypeptides in the presence of ATP. B, TAT-NSF81 inhibits NSF disassembly activity. Increasing amounts of recombinant NSF were pretreated with TAT-NSF81 for 20 min, mixed with α-SNAP and SNARE fusion polypeptides as above. ATP was added, SNAREs were precipitated as above, and the precipitant was analyzed for the coprecipitation of NSF. C, TAT-NSF81scr control does not inhibit NSF disassembly activity. Increasing amounts of recombinant NSF were pretreated with TAT-NSF81scr as described above, and NSF disassembly activity was assayed as above. D, TAT-NSF700 inhibits NSF disassembly activity. Increasing amounts of recombinant NSF were pretreated with TAT-NSF700 as above, and NSF disassembly activity was assayed as described above. E, TAT-NSF700scr control peptide does not inhibit NSF disassembly activity. Increasing amounts of recombinant NSF were pretreated with TAT-NSF700scr as described above, and NSF disassembly activity was assayed as above.

NSF57 at inhibiting NSF disassembly of the SNARE complex (Fig. 4). Because NSF hydrolysis of ATP is important for NSF disassembly of SNARE complexes, it is not surprising that the TAT-NSF polypeptides that inhibit NSF ATPase activity also inhibit NSF disassembly activity (Fig. 4).

NSF forms homohexamers in a barrel-shaped ring structure that is important for NSF function (Yu et al., 1998; Zhang et al., 2000). We designed a peptide TAT-NSF700 that interferes with NSF interactions with other NSF molecules. However, we do not have a robust assay to detect NSF homohexamerization. Although TAT-NSF700 was the most potent inhibitor of exocytosis, the precise mechanism of its action is not yet known.

TAT-NSF Entry into Endothelial Cells. TAT polypeptides enter cells by macropinocytosis (Wadia et al., 2004). The composition of the TAT amino acid residues that affects the α-helical structure of the TAT domain influences TAT uptake into cells (Ho et al., 2001). Furthermore, the composition of the NSF domain of the fusion polypeptides may also affect cellular uptake. Most of the TAT-NSF fusion polypeptides transduce similar percentages of endothelial cells (Fig. 2B). However, the concentration of TAT-NSF peptides within cells after 20 min varies by approximately 20% (Fig. 2A, ■). For example, TAT-NSF57 and TAT-NSF700 achieve higher levels within endothelial cells compared with the other peptides (Fig. 2A, ■). One possible explanation for this difference is that the amino acids in the NSF domain affect TAT-NSF peptide entry into cells. Another possibility is that more FITC molecules are attached to TAT-NSF700 and TAT-NSF57 than to the other TAT-NSF peptides (Fig. 2A, □).

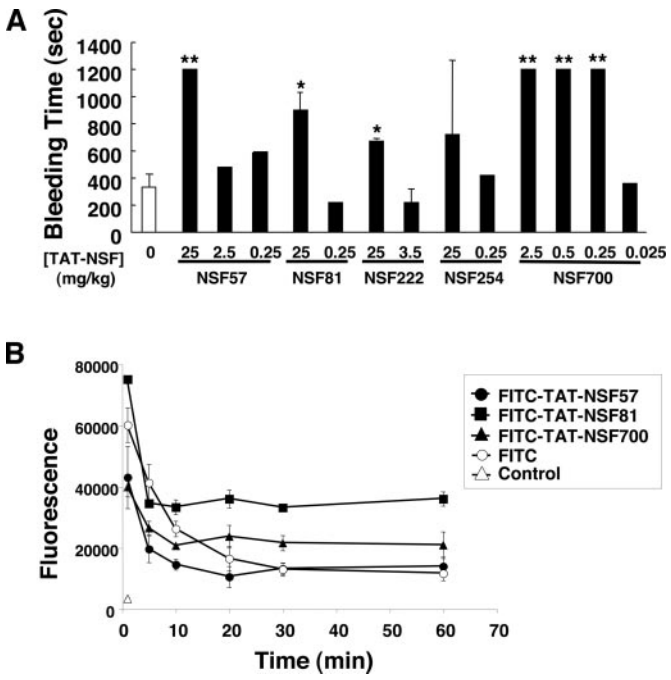

Fig. 5. Effect of TAT-NSF peptides on bleeding time in mice. A, bleeding times. Mice were injected intravenously with PBS or the TAT-NSF peptides (in nanomoles per gram), and after 45 min, the distal tip of the tail was amputated, and the bleeding time was measured ($n = 3 \pm$ S.D.; ⋆, $P < 0.05$ versus 0 mg/kg; ⋆⋆, $P < 0.01$ versus 0 mg/kg). Bleeding for longer than 20 min was scored as 20 min. B, bioavailability of TAT-NSF peptides in mice. Mice were injected intravenously with PBS, FITC, or 0.5 mg/kg FITC-TAT-NSF peptides, and the distal tip of the tail was amputated and blood collected at various times. Fluorescence in the blood were measured by fluorometry ($n = 3 \pm$ S.D.).

However, TAT-NSF81 has a higher fluorescence than the other peptides yet has lower levels within cells. Thus FITC-labeling alone cannot account for the entire difference in TAT-NSF levels within cells.

TAT-NSF Peptides Inhibit Exocytosis. The TAT-NSF peptides inhibit exocytosis in endothelial cells. Each set of dose responses was performed with a given lot of endothelial cells. However, the batch of endothelial cells used for one peptide differs from the cells used for another peptide. This may account for the variation in vWF release at baseline (Fig. 1). Our data suggest that the mechanism by which the peptides inhibit exocytosis is by acting on NSF, a protein that plays a critical role in exocytosis (Block et al., 1988; Malhotra et al., 1988; Rothman, 1994). We also explored the effect of TAT-NSF peptides in insulinoma cells that release insulin by exocytosis. TAT-NSF peptides inhibit insulinoma release of insulin (Fig. 1D). These data suggest that TAT-NSF peptides may be useful in the inhibition of exocytosis in a variety of cells.

How Do TAT-NSF Peptides Prolong Bleeding Time? Our novel set of NSF inhibitors prolonged bleeding times in mice (Fig. 5), but the precise mechanisms are unknown. We hypothesize that TAT-NSF peptides act on endothelial cells, because TAT-NSF peptides cannot enter platelets (data not shown). We further hypothesize that TAT-NSF peptides then inhibit NSF and thereby block endothelial exocytosis of Weibel-Palade bodies from vascular endothelial cells, as supported by our data (Figs. 1–4). Endothelial cells would then externalize less P-selectin and release less vWF. Less P-selectin on the surface of endothelial cells would decrease platelet adherence to the vessel wall mediated by the platelet surface-protein P-selectin glycoprotein ligand-1 (Andre et al., 2000). Less vWF released into the blood would decrease platelet adherence to the vessel wall mediated by the platelet glycoprotein Ib-IX-V receptor complex (Ruggeri, 2002). The combined effects of decreased endothelial release of these mediators would, in theory, lead to decreased platelet adhesion to the vessel wall and thereby prolong the time to hemostasis (Fig. 5).

TAT-NSF Concentrations in Mouse Blood. The blood levels of FITC-TAT-NSF decrease rapidly over the first 5 min after injection and then do not change from 10 min after injection until at least 60 min after injection (Fig. 5B). The cause of the steep initial decrease in blood concentrations of FITC-TAT-NSF is unclear. It is possible that the FITC-TAT-NSF peptides are taken up rapidly by vascular cells (including endothelial cells and leukocytes). Endothelial cells take up FITC-TAT-NSF within 20 min of exposure ex vivo (Fig. 2A). Factors influencing the constant levels of FITC-TAT-NSF between 10 and 60 min after administration are also unclear. One possibility is that the FITC-TAT-NSF peptides can achieve a steady state within endothelial cells, with equal amounts of peptide entering and exiting cells.

The initial blood concentration of FITC-TAT-NSF81 is higher than the other peptides (Fig. 5B). The reason for this is unclear. FITC-TAT-NSF81 has higher levels of fluorescence than other FITC-TAT-NSF peptides in media alone (Fig. 2A, □). FITC-TAT-NSF81 has lower concentrations within cells ex vivo (Fig. 2A, ■). Thus, it is possible that FITC-TAT-NSF81 has a higher basal level of fluorescence in vivo and does not enter cells as rapidly in vivo, compared

with the other FITC-TAT-NSF peptides, thus causing a higher initial level of fluorescence in vivo.

We also explored the effect of TAT-NSF peptides on the bleeding time when administered intraperitoneally instead of intravenously. Although prior reports suggested that the protein transduction domain of TAT permits delivery of fusion polypeptides throughout the body, we found that TAT-NSF peptides have no effect on bleeding time when administered intraperitoneally (data not shown). These results suggest that TAT-NSF fusion polypeptides administered intravenously remain in the vascular compartment and may only inhibit exocytosis of vascular cells. Modification of the amino-terminal tag of TAT-NSF polypeptides may permit targeting of specific secretory cells outside of the vascular compartment.

Implications for Treatment of Diseases. Exocytosis may play a role in a variety of diseases. Excessive release of granules from endothelial cells, platelets, or cytotoxic T lymphocytes may contribute to the pathophysiology of thrombosis, stroke, or autoimmunity. The polypeptide inhibitors of exocytosis described in this report may represent a novel treatment for a select group of diseases in which excess exocytosis plays a pathophysiological role.

Acknowledgments

We gratefully acknowledge Dr. Theresa Shapiro for advice and for assistance in calculating the EC_{50} values for the TAT-NSF peptides.

References

Andre P, Denis CV, Ware J, Saffaripour S, Hynes RO, Ruggeri ZM, and Wagner DD (2000) Platelets adhere to and translocate on von Willebrand factor presented by endothelium in stimulated veins. *Blood* **96:**3322–3328.

Becker-Hapak M, McAllister SS, and Dowdy SF (2001) TAT-mediated protein transduction into mammalian cells. *Methods* **24:**247–256.

Birch KA, Ewenstein BM, Golan DE, and Pober JS (1994) Prolonged peak elevations in cytoplasmic free calcium ions, derived from intracellular stores, correlate with the extent of thrombin-stimulated exocytosis in single human umbilical vein endothelial cells. *J Cell Physiol* **160:**545–554.

Block MR, Glick BS, Wilcox CA, Wieland FT, and Rothman JE (1988) Purification of an N-ethylmaleimide-sensitive protein catalyzing vesicular transport. *Proc Natl Acad Sci USA* **85:**7852–7856.

Dalal S and Hanson PI (2001) Membrane traffic: what drives the AAA motor? *Cell* **104:**5–8.

Datta YH, Romano M, Jacobson BC, Golan DE, Serhan CN, and Ewenstein BM (1995) Peptido-leukotrienes are potent agonists of von Willebrand factor secretion and P-selectin surface expression in human umbilical vein endothelial cells. *Circulation* **92:**3304–3311.

Ferro-Novick S and Jahn R (1994) Vesicle fusion from yeast to man. *Nature (Lond)* **370:**191–193.

Foreman KE, Vaporciyan AA, Bonish BK, Jones ML, Johnson KJ, Glovsky MM, Eddy SM, and Ward PA (1994) C5a-induced expression of P-selectin in endothelial cells. *J Clin Investig* **94:**1147–1155.

Ho A, Schwarze SR, Mermelstein SJ, Waksman G, and Dowdy SF (2001) Synthetic protein transduction domains: enhanced transduction potential in vitro and in vivo. *Cancer Res* **61:**474–477.

Huang TG and Hackney DD (1994) *Drosophila* kinesin minimal motor domain expressed in *Escherichia coli*. Purification and kinetic characterization. *J Biol Chem* **269:**16493–16501.

Malhotra V, Orci L, Glick BS, Block MR, and Rothman JE (1988) Role of an N-ethylmaleimide-sensitive transport component in promoting fusion of transport vesicles with cisternae of the Golgi stack. *Cell* **54:**221–227.

Matsushita K, Morrell CN, Cambien B, Yang SX, Yamakuchi M, Bao C, Hara MR, Quick RA, Cao W, O'Rourke B, et al. (2003) Nitric oxide regulates exocytosis by S-nitrosylation of N-ethylmaleimide-sensitive factor. *Cell* **115:**139–150.

Matveeva EA, He P, and Whiteheart SW (1997) *N*-Ethylmaleimide-sensitive fusion protein contains high and low affinity ATP-binding sites that are functionally distinct. *J Biol Chem* **272:**26413–26418.

May AP, Misura KM, Whiteheart SW, and Weis WI (1999) Crystal structure of the amino-terminal domain of N-ethylmaleimide-sensitive fusion protein. *Nat Cell Biol* **1:**175–182.

Nagiec EE, Bernstein A, and Whiteheart SW (1995) Each domain of the *N*-ethylmaleimide-sensitive fusion protein contributes to its transport activity. *J Biol Chem* **270:**29182–29188.

Pallanck L, Ordway RW, and Ganetzky B (1995) A *Drosophila* NSF mutant. *Nature (Lond)* **376:**25.

Pevsner J, Hsu SC, and Scheller RH (1994) n-Sec1: a neural-specific syntaxin-binding protein. *Proc Natl Acad Sci USA* **91:**1445–1449.

Rothman JE (1994) Mechanisms of intracellular protein transport. *Nature (Lond)* **372:**55–63.

Ruggeri ZM (2002) Platelets in atherothrombosis. *Nat Med* **8:**1227–1234.

Schwarze SR, Ho A, Vocero-Akbani A, and Dowdy SF (1999) In vivo protein transduction: delivery of a biologically active protein into the mouse. *Science (Wash DC)* **285:**1569–1572.

Sollner T, Bennett MK, Whiteheart SW, Scheller RH, and Rothman JE (1993a) A protein assembly-disassembly pathway in vitro that may correspond to sequential steps of synaptic vesicle docking, activation and fusion. *Cell* **75:**409–418.

Sollner T, Whiteheart SW, Brunner M, Erdjument-Bromage H, Geromanos S, Tempst P, and Rothman JE (1993b) SNAP receptors implicated in vesicle targeting and fusion. *Nature (Lond)* **362:**318–324.

Steel GJ and Morgan A (1998) Selective stimulation of the D1 ATPase domain of N-ethylmaleimide- sensitive fusion protein (NSF) by soluble NSF attachment proteins. *FEBS Lett* **423:**113–116.

Tagaya M, Wilson DW, Brunner M, Arango N, and Rothman JE (1993) Domain structure of an N-ethylmaleimide-sensitive fusion protein involved in vesicular transport. *J Biol Chem* **268:**2662–2666.

Utgaard JO, Jahnsen FL, Bakka A, Brandtzaeg P, and Haraldsen G (1998) Rapid secretion of prestored interleukin 8 from Weibel-Palade bodies of microvascular endothelial cells. *J Exp Med* **188:**1751–1756.

Vischer UM, Jornot L, Wollheim CB, and Theler JM (1995) Reactive oxygen intermediates induce regulated secretion of von Willebrand factor from cultured human vascular endothelial cells. *Blood* **85:**3164–3172.

Vischer UM and Wollheim CB (1997) Epinephrine induces von Willebrand factor release from cultured endothelial cells: involvement of cyclic AMP-dependent signalling in exocytosis. *Thromb Haemost* **77:**1182–1188.

Vocero-Akbani A, Chellaiah MA, Hruska KA, and Dowdy SF (2001) Protein transduction: delivery of Tat-GTPase fusion proteins into mammalian cells. *Methods Enzymol* **332:**36–49.

Vocero-Akbani A, Lissy NA, and Dowdy SF (2000) Transduction of full-length Tat fusion proteins directly into mammalian cells: analysis of T cell receptor activation-induced cell death. *Methods Enzymol* **322:**508–521.

Wadia JS, Stan RV, and Dowdy SF (2004) Transducible TAT-HA fusogenic peptide enhances escape of TAT-fusion proteins after lipid raft macropinocytosis. *Nat Med* **10:**310–315.

Wagner DD (1993) The Weibel-Palade body: the storage granule for von Willebrand factor and P-selectin. *Thromb Haemost* **70:**105–110.

Weber T, Zemelman BV, McNew JA, Westermann B, Gmachl M, Parlati F, Sollner TH, and Rothman JE (1998) SNAREpins: minimal machinery for membrane fusion. *Cell* **92:**759–772.

Weiss EJ, Hamilton JR, Lease KE, and Coughlin SR (2002) Protection against thrombosis in mice lacking PAR3. *Blood* **100:**3240–3244.

Whiteheart SW, Rossnagel K, Buhrow SA, Brunner M, Jaenicke R, and Rothman JE (1994) N-ethylmaleimide-sensitive fusion protein: a trimeric ATPase whose hydrolysis of ATP is required for membrane fusion. *J Cell Biol* **126:**945–954.

Whiteheart SW, Schraw T, and Matveeva EA (2001) N-ethylmaleimide sensitive factor (NSF) structure and function. *Int Rev Cytol* **207:**71–112.

Wolff B, Burns AR, Middleton J, and Rot A (1998) Endothelial cell "memory" of inflammatory stimulation: human venular endothelial cells store interleukin 8 in Weibel-Palade bodies. *J Exp Med* **188:**1757–1762.

Yu RC, Hanson PI, Jahn R, and Brunger AT (1998) Structure of the ATP-dependent oligomerization domain of *N*-ethylmaleimide sensitive factor complexed with ATP. *Nat Struct Biol* **5:**803–811.

Zhang X, Shaw A, Bates PA, Newman RH, Gowen B, Orlova E, Gorman MA, Kondo H, Dokurno P, Lally J, et al. (2000) Structure of the AAA ATPase p97. *Mol Cell* **6:**1473–1484.

Address correspondence to: Dr. Charles J. Lowenstein, 950 Ross Building, 720 Rutland Avenue, The Johns Hopkins University School of Medicine, Baltimore, MD 21205. E-mail: clowenst@jhmi.edu